RSC Advances

PAPER

View Article Online
View Journal | View Issue

Cite this: *RSC Adv.*, 2022, **12**, 437

Supported copper on a diamide–diacid-bridged PMO: an efficient hybrid catalyst for the cascade oxidation of benzyl alcohols/Knoevenagel condensation†

Ehsan Valiey and Mohammad G. Dekamin *

In this study, a novel periodic mesoporous organosilica (PMO) containing diamide–diacid bridges was conveniently prepared using ethylenediaminetetraacetic dianhydride to support Cu(II) species and affording supramolecular Cu@EDTAD-PMO nanoparticles efficiently. Fourier transform infrared (FT-IR) and energy dispersive X-ray (EDX) spectroscopy, thermogravimetric analysis (TGA), X-ray diffraction (XRD), field emission scanning electron microscopy (FESEM), Brunauer–Emmett–Teller (BET) analysis, and high-resolution transmission electron microscopy (HRTEM) results confirmed the successful synthesis of Cu@EDTAD-PMO. The stabilized Cu(II) nanoparticles inside the mesochannels of the new PMO provided appropriate sites for selective oxidation of different benzyl alcohol derivatives to their corresponding benzaldehydes and subsequent Knoevenagel condensation with malononitrile. Therefore, Cu@EDTAD-PMO can be considered as a multifunctional heterogeneous catalyst, which is prepared easily through a green procedure and demonstrates appropriate stability with almost no leaching of the Cu(II) nanoparticles into the reaction medium, and easy recovery through simple filtration. The recycled Cu@EDTAD-PMO was reused up to five times without significant loss of its catalytic activity. The stability, recoverability, and reusability of the designed heterogeneous catalyst were also studied under various reaction conditions.

Received 29th August 2021
Accepted 7th December 2021

DOI: 10.1039/d1ra06509b

rsc.li/rsc-advances

Introduction

Mesoporous silica has long been known as a popular subject for research in materials science due to its special properties from both morphology and surface chemistry points of view. Nanostructured mesoporous materials have features such as high specific surface area, regular pore channels, high permeability, large pore volume, and high tolerability.[1–14] By controlling the assembly or growth processes, different types of products with various structures, morphologies, or particle sizes can be produced.[12,13,15–21]

Periodic mesoporous organosilicas (PMOs) were first reported in 1999 by Inagaki,[22] Ozin,[23] and Stein.[24] They are a class of materials synthesized *via* a sol–gel process from an organo-bridged alkoxysilane in the presence of a surfactant. PMO materials can be prepared in the nanoscale; this property is very important especially for potential applications such as drug-release,[25–33] sensors, chromatography, catalysis, and adsorption purposes.[20,28,34,35] Generally, the organosiloxane bridges determine the physical and chemical properties of the corresponding PMOs. Also, PMOs are characterized by their high specific surface area and ordered mesopores. Hence, PMOs are very desirable in the field of green catalysis.[29,30,34,36,37] In addition, PMOs can graft or support catalytically active centers such as Brønsted acids as well as transition metals.[37–40] Ethylenediamine tetraacetic acid (EDTA) is widely used as a strong complexing agent. EDTA is a multidentate ligand with six binding sites including four carboxyl and two amino groups. Consequently, EDTA forms a cage-like structure around the metal ions to afford corresponding metal–ligand complexes, which are extremely stable. On the other hand, ethylenediaminetetraacetic dianhydride (EDTAD), a derivative of EDTA comprising two anhydride groups, can react with amine and hydroxyl groups of other compounds. EDTAD is used in various applications such as baker's yeast biomass treatment for producing biosorbents with a high capacity for the adsorption of Cu(II) and Pb(II) ions.[41] Also, EDTA has been grafted on various structures such as graphene oxides,[42] polymers,[43,44] MOFs,[45] or mesoporous silica[46] to adsorb metal ions. However, designing of more effective PMOs containing organic moieties including EDTA with stronger metal–ligand interactions is still in demand.

Copper is a suitable metal compared to other transition metals for many oxidation reactions, due to its natural

Pharmaceutical and Heterocyclic Compounds Research Laboratory, Department of Chemistry, Iran University of Science and Technology, Tehran, 16846-13114, Iran. E-mail: mdekamin@iust.ac.ir

† Electronic supplementary information (ESI) available. See DOI: 10.1039/d1ra06509b

abundance, low toxicity, and oxidation potential. Therefore, supramolecular chelating of Cu(II) species onto the surface of PMO which enhances their catalytic activity would be very desirable. This will provide successful examples of the sustainable catalysis and one-pot multistep synthesis. Actually, one-pot multistep reactions, also known as cascade reactions, do not require isolation of intermediates and reduce the solvent waste. Hence, cascade reactions have recently attracted attention in both industry and laboratory.[47–52] These reactions provide products in very good to excellent yields and therefore follow the principles of green chemistry and sustainable chemistry.

Cyanocinamonitriles, which are prepared *via* Knoevenagel condensation of a carbonyl group and a C–H acid, can act as a multifunctional intermediate in the synthesis of important chemicals.[53–60] Nowadays, the sequential oxidation of alcohols and the subsequent Knoevenagel condensation reaction of the obtained aldehyde compounds has received much attention in terms of green and sustainable standpoints of view compared to the classical multi-step reactions.[16,61–66] Traditionally, stoichiometric amounts of oxidants such as chromium reagents,[67] Dess–Martin periodinane,[68,69] or permanganates[70] are used for oxidation of alcohols. These oxidants have adverse environmental impacts due to their toxicity and large amounts of waste. Hence, designing of efficient catalytic systems based on low toxic catalytic species and oxidants can address these challenges. In this research, the preparation and characterization of novel Cu(II) species on ethylenediaminetetraacetic-bridged periodic mesoporous organosilica (Cu@EDTAD-PMO) is reported, as a recyclable catalyst, for the cascade oxidation/Knoevenagel condensation of benzyl alcohols with malononitrile using *tert*-butyl hydroperoxide (TBHP) as a green oxidant (Scheme 1).

Results and discussion

The prepared Cu@EDTAD-PMO mesoporous organosilica (**1**) was characterized by using spectroscopic, microscopic or analytical methods including FTIR, EDX, FESEM, HRTEM, XRD, TGA and BET analysis. FTIR spectra of the Cu@EDTAD-PMO mesoporous (**1**) along with its precursor (EDTAD-PMO) shown in Fig. 1 confirm the existence of both Cu(II) species and EDTAD. Absorption bands at 3000–3600 and 2928 cm^{-1} belong to the stretching vibrations of O–H bonds of hydroxyl groups and the stretching vibration of C–H aliphatic bonds, respectively. The absorption bands at 1700 and 1664 cm^{-1} are attributed to the acid groups and amide groups, respectively. The Si–O vibration was observed at 1000–1200 cm^{-1} (Fig. 1a). Furthermore, in Fig. 1b the characteristic band for Cu–NH stretching vibrations was observed at 700–800 cm^{-1}. Also, the recycled catalyst from the model reaction after six consecutive runs was studied using FTIR spectroscopy, which showed appropriate stability of the Cu@EDTAD-PMO mesoporous organosilica (**1**) as a heterogeneous catalyst.

EDX spectra of the EDTAD-PMO and Cu@EDTAD-PMO (**1**) are illustrated in Fig. 2. It can be seen that the EDTAD-PMO is composed of C, N, O and Si atoms (Fig. 2a) while the synthesized Cu@EDTAD-PMO (**1**) consists mainly of C, N, O, Si and Cu atoms or species (Fig. 2b). In addition, EDX mapping was carried out to observe the distribution of the elements in the

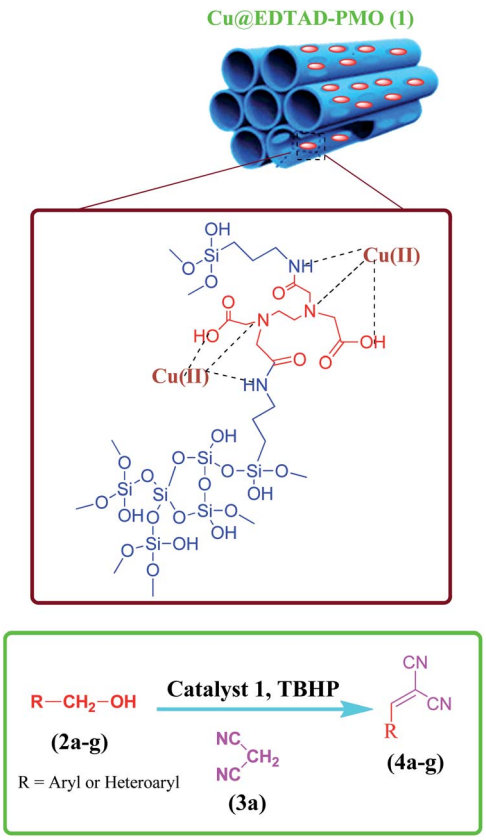

Scheme 1 Cu@EDTAD-PMO (**1**)-catalyzed cascade oxidation/Knoevenagel condensation of benzyl alcohols with malononitrile using *tert*-butyl hydroperoxide (TBHP) as a green oxidant.

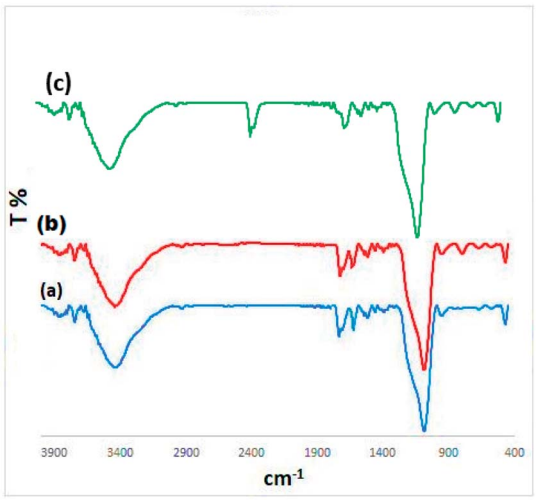

Fig. 1 FTIR spectra of the EDTAD-PMO (a), fresh Cu@EDTAD-PMO mesoporous catalyst (**1**, (b)) and the recycled catalyst after six consecutive runs (c).

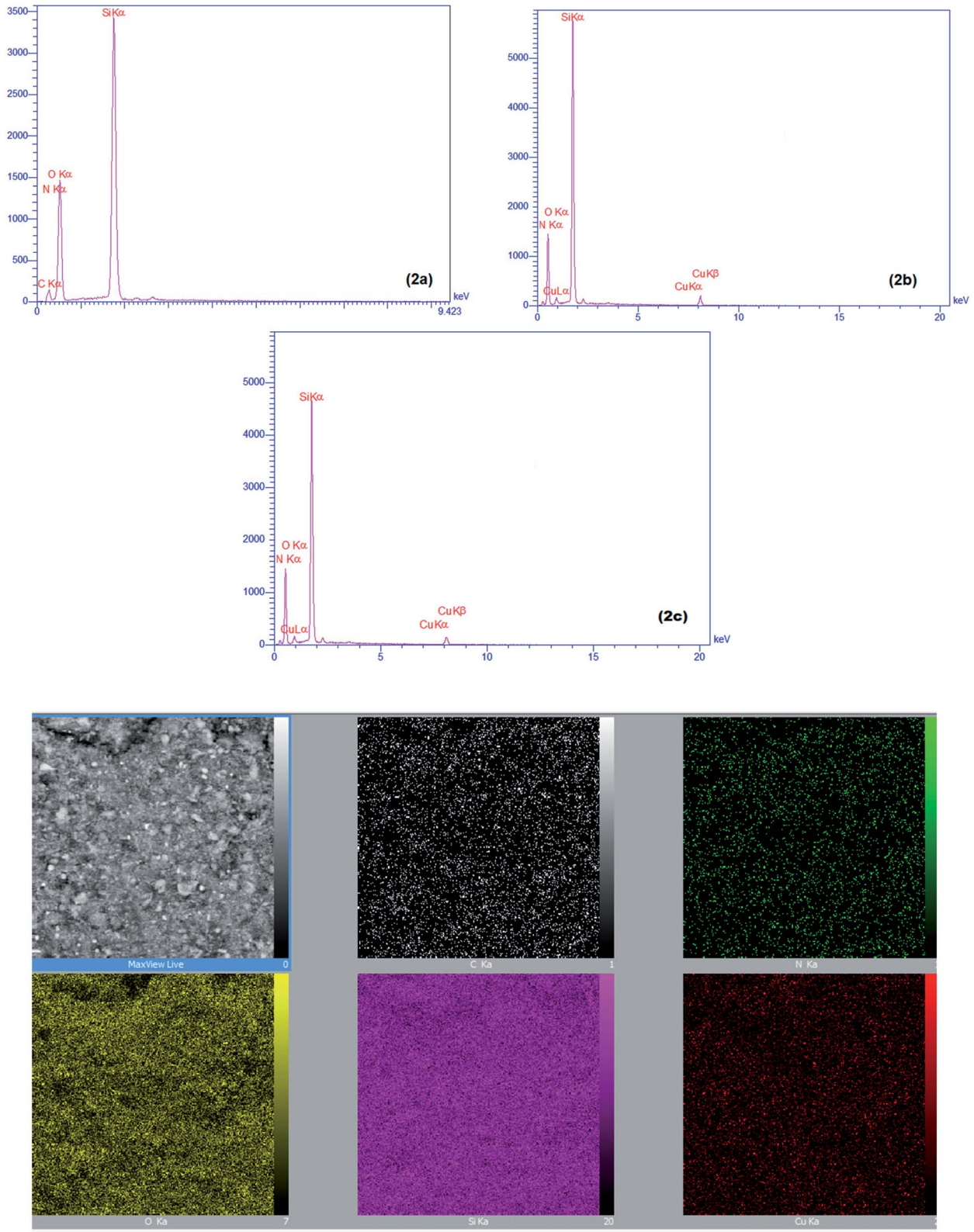

Fig. 2 EDX spectra of the EDTAD-PMO (2a), fresh Cu@EDTAD-PMO (**1**, (2b)) and the recycled Cu@EDTAD-PMO catalyst (**1**) from the model reaction after six consecutive runs (**1**, (2c)) along with the elemental mapping of the fresh Cu@EDTAD-PMO (**1**).

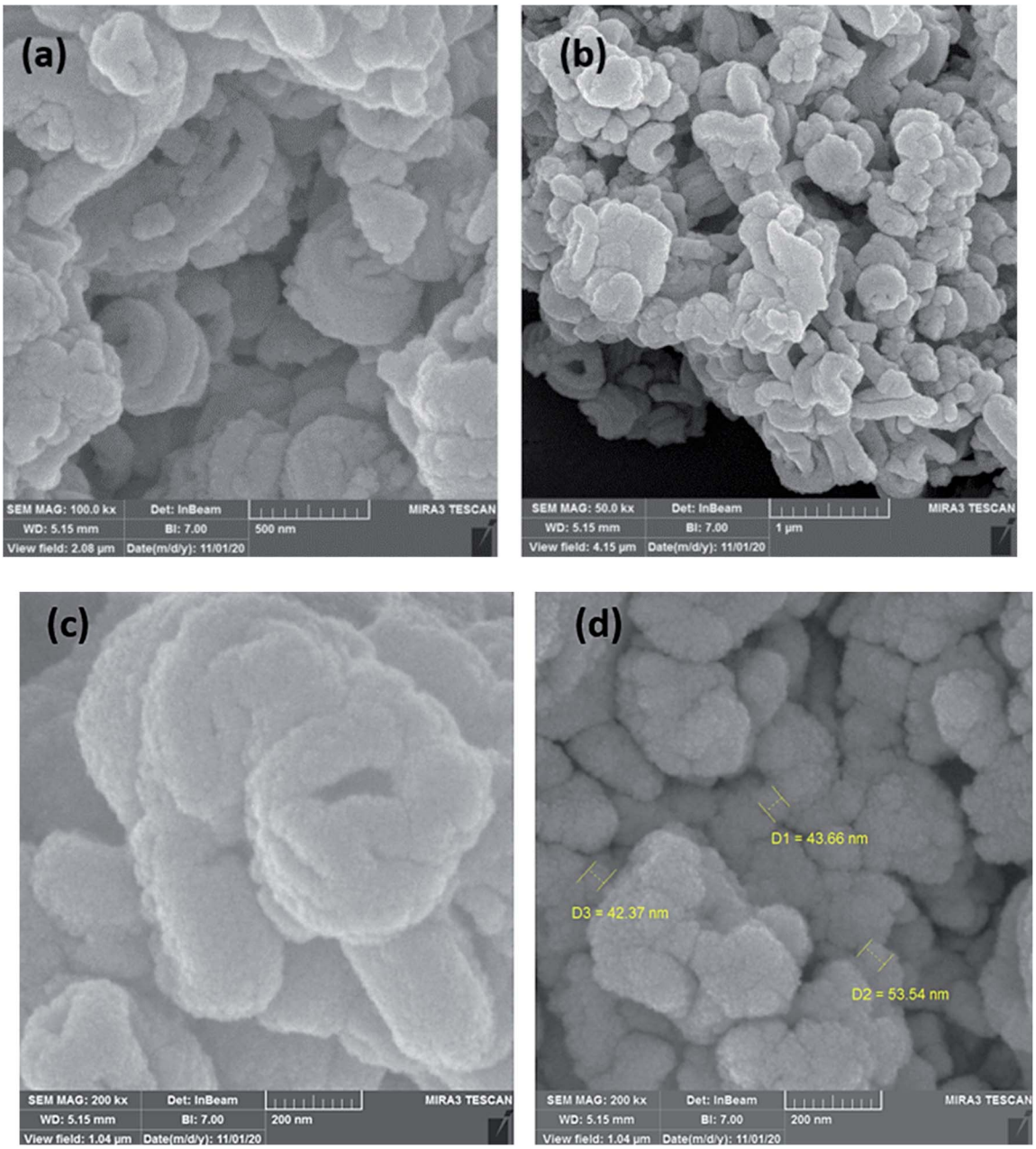

Fig. 3 FESEM images of the Cu@EDTAD-PMO nano-ordered catalyst (**1**) with different magnifications (a–d).

Cu@EDTAD-PMO (**1**). As can be seen in Fig. 2b, the detected elements, especially Cu species, show uniform distribution. Also, Fig. 2c is related to the EDX spectra of recycled catalyst from the model reaction after six consecutive runs. In addition, ICP-AES analysis of the Cu@EDTAD-PMO (**1**) indicated that the amount of Cu(II) species is about 2.1 mmol g^{-1}. Furthermore, ICP-AES analysis of the recycled Cu@EDTAD-PMO (**1**) indicated that the amount of Cu is about 1.98×10^{-3} mol g^{-1}.

The morphology and particle size of Cu@EDTAD-PMO (**1**) were examined by FESEM and HRTEM techniques (Fig. 3 and 4). FESEM images of Cu@EDTAD-PMO (**1**) indicated that it consists of interwoven tubular particles with 42.37–53.54 nm in width (Fig. 3). In addition, the original morphology was retained after the supramolecular chelation of Cu nanoparticles. Also, HRTEM images of Cu@EDTAD-PMO (**1**) revealed the arrangement of mesopores (Fig. 4).

Fig. 5 shows XRD patterns of the Cu@EDTAD-PMO (**1**). Low-angle XRD patterns for the Cu@EDTAD-PMO (**1**) indicated one sharp peak at $2\theta = 1.35°$, which arises from the periodicity of the mesoporous structure (Fig. 5a). Moreover, wide-angle diffraction signal at 2θ of 20–30°, the characteristic signal of amorphous SiO_2, is also observed in the XRD pattern of the Cu@EDTAD-PMO nanomaterial (**1**, Fig. 5b). Furthermore, the diffraction peaks at 2θ of 44.30°, 50.30°, and 75° (marked

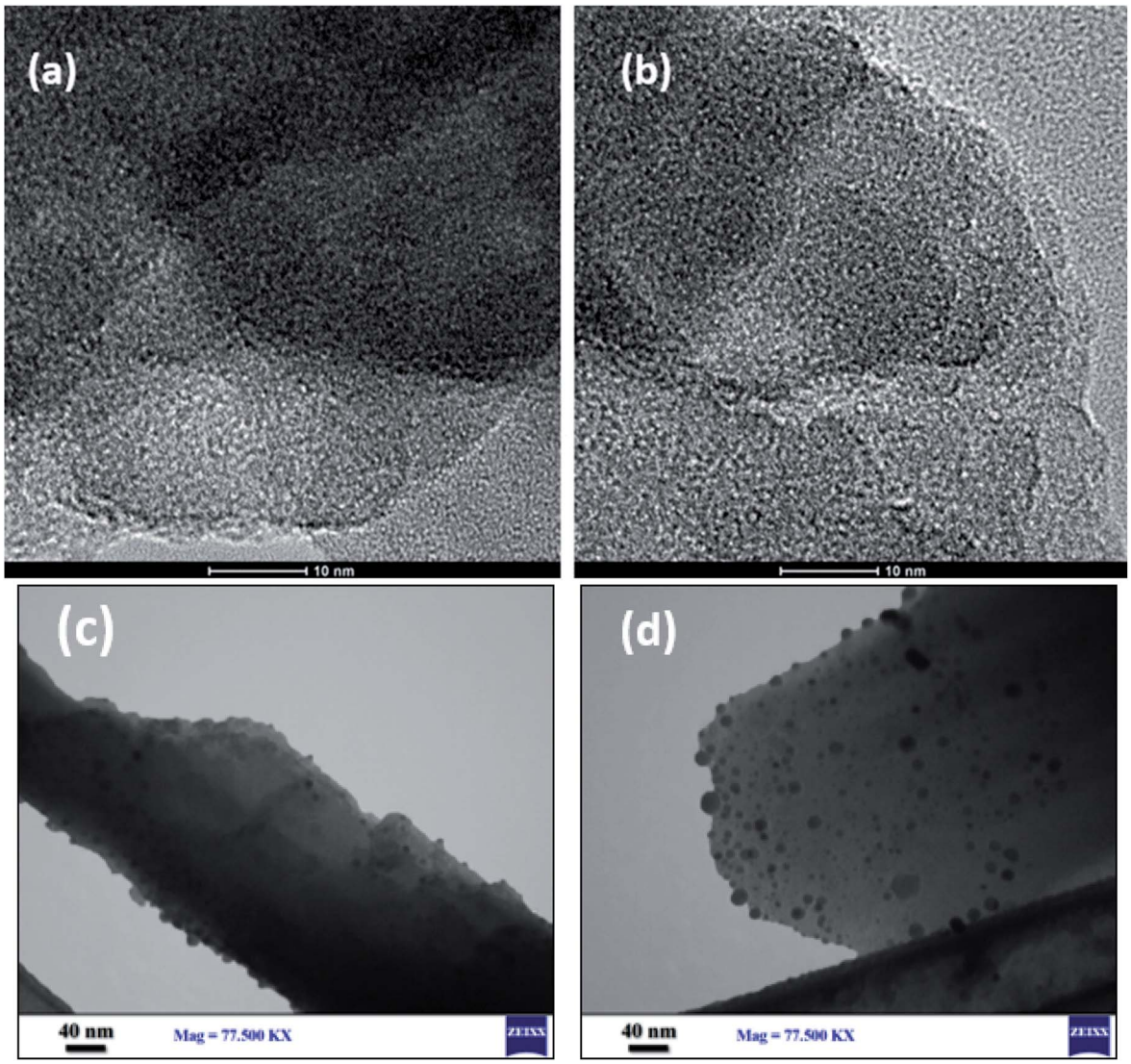

Fig. 4 HRTEM images of the Cu@EDTAD-PMO nano-ordered catalyst (1, a–d).

with ●) can be attributed to the reflections of the Cu species in the structure of mesoporous Cu@EDTAD-PMO (**1**). The stability of the Cu@EDTAD-PMO mesoporous organosilica (**1**) was further confirmed using low-angle XRD pattern observed for the recycled catalyst from the model reaction after six consecutive runs (Fig. 5c).

The mesoporous Cu@EDTAD-PMO (**1**) material was also characterized by TGA and DTA by heating from 50 °C to 800 °C under air flow (Fig. 6). The TGA curve of Cu@EDTAD-PMO shows three weight losses; the first weight loss of about 4 wt% at 50–150 °C due to the evaporation of surface water or solvent molecules adsorbed into the structure of Cu@EDTAD-PMO (**1**), the second weight loss of about 24 wt% from 230 °C to 400 °C due to decomposition of the EDTAD bridging groups, and the third weight loss of about 14 wt% at 450–650 °C due to the coversion of silanol groups to the corresponding siloxane groups. These results also indicate that Cu@EDTAD-PMO (**1**) has been successfully synthesized.

As can be seen in Fig. 7, N_2 adsorption–desorption analysis of the Cu@EDTAD-PMO (**1**) illustrated a type IV isotherm with an H4 hysteresis loop, which is characteristic of mesoporous materials having uniform pore size distribution.[71,72] Indeed, BET (Brunauer–Emmett–Teller) analysis of Cu@EDTAD-PMO (**1**) demonstrated high specific surface area of 623 $m^2\ g^{-1}$ with a total pore volume of 0.44 $cm^3\ g^{-1}$. The BJH (Barrett–Joyner–Halenda) calculations also illustrated highly uniform pore diameter distribution of 6.05 nm.

Cu@EDTAD-PMO-promoted cascade oxidation/Knoevenagel condensation for the synthesis of α,β-unsaturated nitriles 4a–f

To study the catalytic application of Cu@EDTAD-PMO (**1**), the one-pot oxidation/Knoevenagel condensation reactions between benzyl

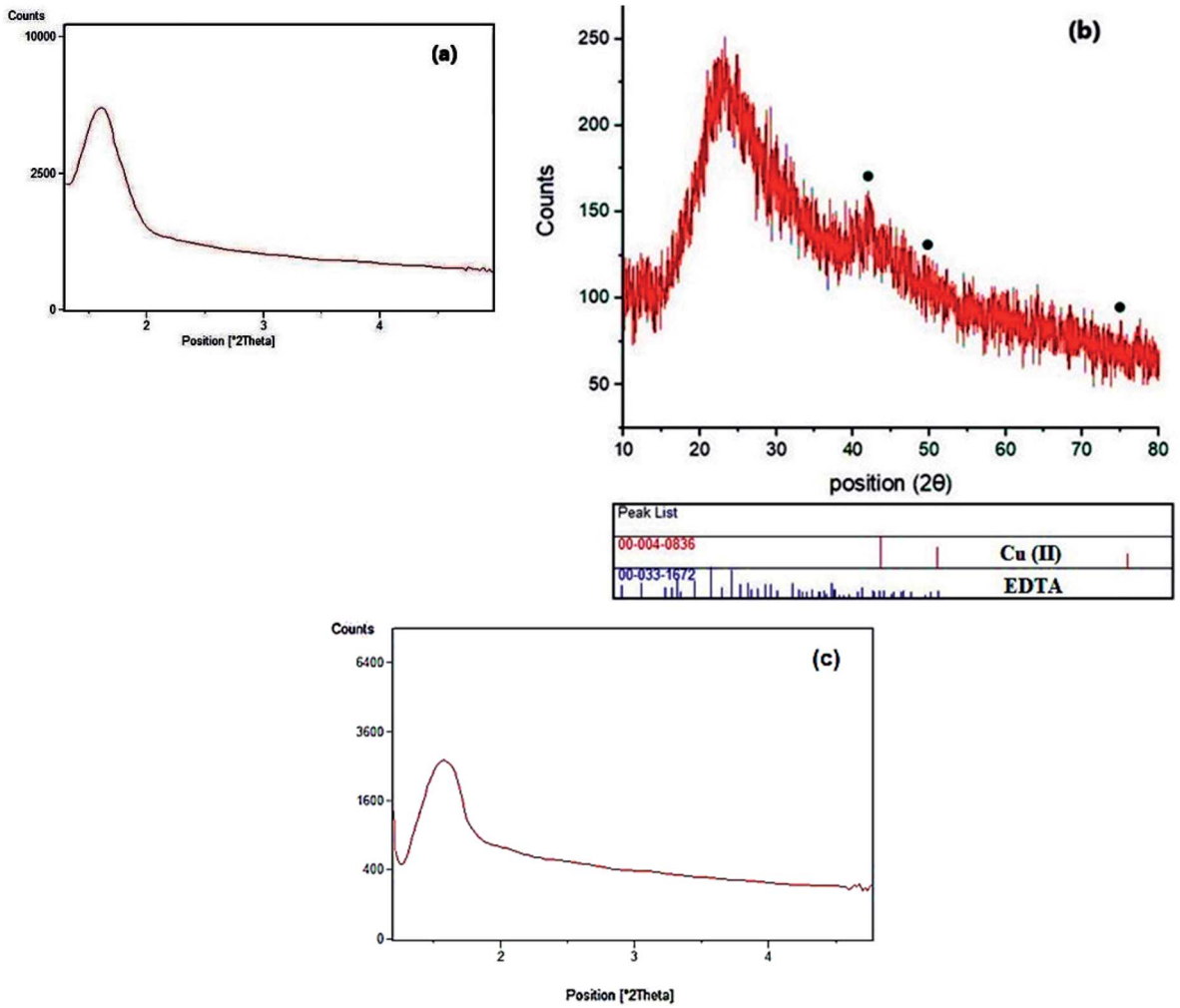

Fig. 5 Low-angle (a) and wide-angle (b) XRD patterns of the fresh Cu@EDTAD-PMO catalyst (**1**), and low-angle XRD pattern of the recycled Cu@EDTAD-PMO catalyst (**1**) from the model reaction after six consecutive runs (c).

alcohol (**2a**) and malononitrile (**3**) in CH_3CN was chosen as the model reaction. As shown in Table 1, in the absence of catalyst (Cu@EDTAD-PMO, **1**) and using various oxidants including O_2, H_2O_2, air, and TBHP, no 2-benzylidinemalononitrile product (**4a**) was obtained at 80 °C. However, 43%, 35%, and 20% conversion to benzaldehyde (**5a**) was observed when H_2O_2, TBHP, and O_2 were

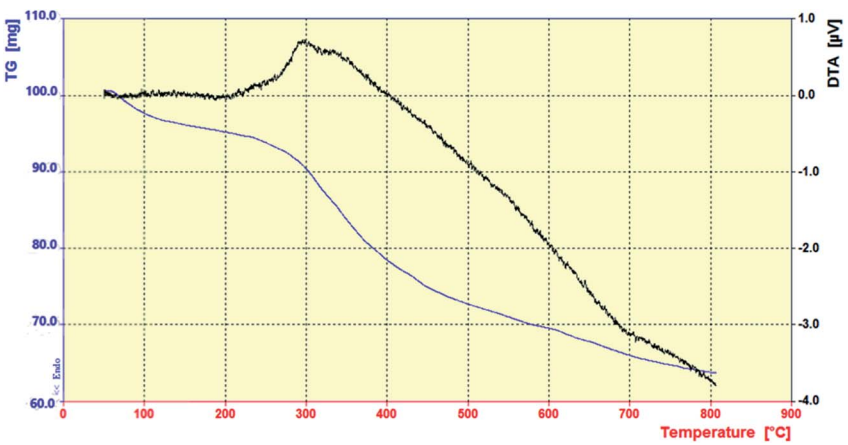

Fig. 6 TGA and DTA curves of the Cu@EDTAD-PMO nanomaterial (**1**).

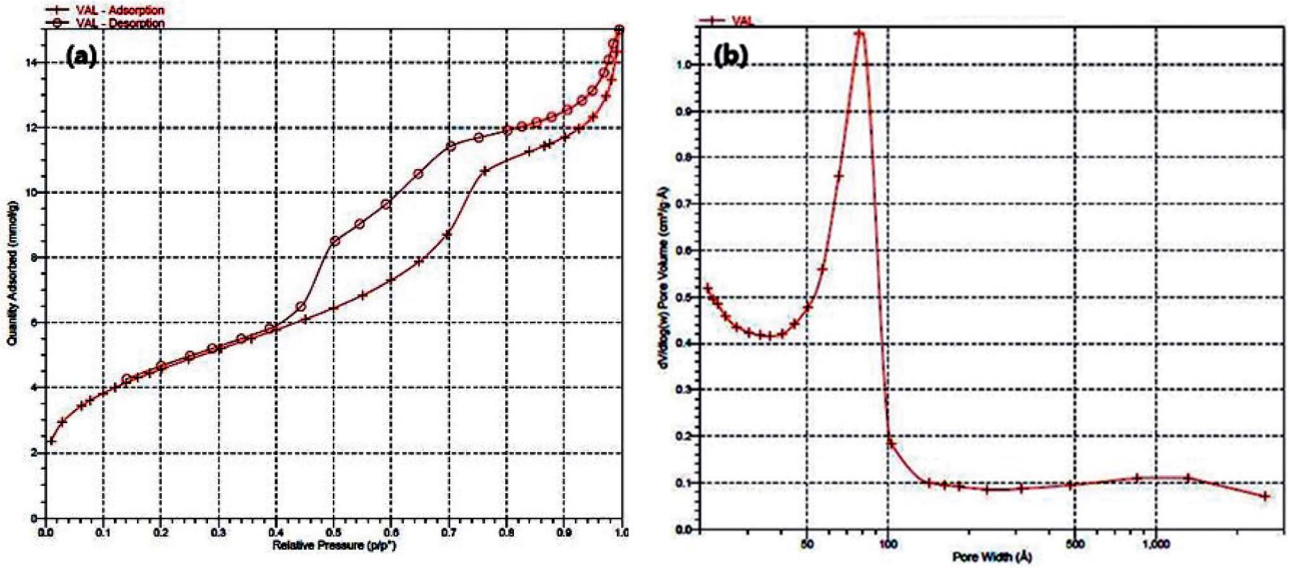

Fig. 7 (a) N_2 adsorption–desorption, and (b) pore size distribution isotherms of the Cu@EDTAD-PMO mesoporous material (**1**).

used, respectively. In addition, only trace amounts of benzaldehyde (**5a**) were produced under air flow (Table 1, entries 1–4). Noteworthy, a yield of about 23% was observed for the favorable benzylidinemalononitrile product (**4a**) by utilizing 2.1 mol% of the Cu@EDTAD-PMO (**1**), as a catalyst, without any oxidant (Table 1, entry 5). TBHP was found to be more efficient than H_2O_2 for the cascade reaction (Table 1, entries 6–7). Actually, the *t*-BuOO radical produced by TBHP is a stronger oxidant than the hydroxyl radical generated by H_2O_2 during the reaction. Indeed, it has been previously reported that OH radicals react with EDTA and cause its

Table 1 Optimization of different conditions for the oxidation/Knoevenagel condensation of benzyl alcohol (**2a**)[a]

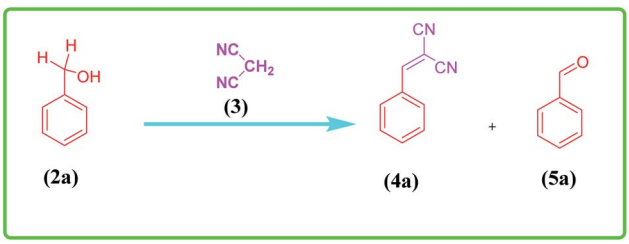

Entry	Catalyst	Catalyst loading (mol%)	Oxidant	Solvent	Temperature (°C)	Time (h)	Yield of (%) **4a**	Yield of (%) **5a**
1	—	—	O_2	CH_3CN	80	24	Trace	20
2	—	—	H_2O_2	CH_3CN	80	24	—	43
3	—	—	Air	CH_3CN	80	24	—	Trace
4	—	—	TBHP	CH_3CN	80	24	—	35
5	Cu@EDTAD-PMO (**1**)	2.1	—	CH_3CN	80	24	23	Trace
6	Cu@EDTAD-PMO (**1**)	2.1	TBHP	CH_3CN	80	10	64	—
7	Cu@EDTAD-PMO (**1**)	2.1	H_2O_2	CH_3CN	80	9	16	Trace
8	Cu@EDTAD-PMO (**1**)	2.1	TBHP	CH_3CN	50	11	70	—
9	Cu@EDTAD-PMO (**1**)	2.1	TBHP	CH_3CN	r.t.	13	65	—
10	Cu@EDTAD-PMO (**1**)	2.1	TBHP	Toluene	50	15	58	—
11	Cu@EDTAD-PMO (**1**)	2.1	TBHP	H_2O	50	20	34	27
12	Cu@EDTAD-PMO (**1**)	1.1	TBHP	CH_3CN	50	10	70	—
13	Cu@EDTAD-PMO (**1**)	3.2	TBHP	CH_3CN	50	8	87	—
14	Cu@EDTAD-PMO (**1**)	4.2	TBHP	CH_3CN	50	6	95	—
15	$Cu(OAc)_2$	4.2	TBHP	CH_3CN	50	6	30	12

[a] Reaction conditions: benzyl alcohol (**2a**, 1 mmol), oxidant (1 mmol), and Cu@EDTAD-PMO (**1**) were added into CH_3CN (2 mL) and stirred at 50 °C unless otherwise stated. Then, malononitrile (**3**, 1.1 mmol) was added to the reaction mixture.

Table 2 Cascade oxidation/Knoevenagel condensation of different benzyl alcohols **2a–f** catalyzed by the Cu@EDTAD-PMO (**1**) under optimized conditions[a]

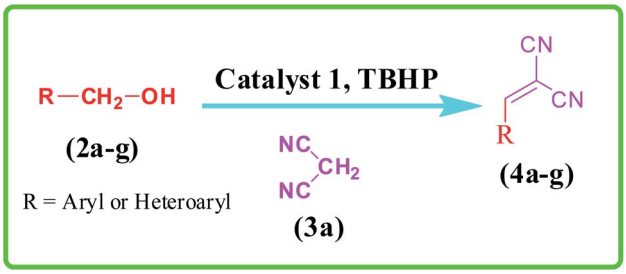

Entry	Substrate 2	Product	Time (h)	Yield (%)
1	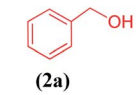 (2a)	 (4a)	6	95
2	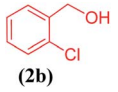 (2b)	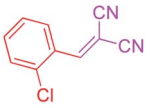 (4b)	10	90
3	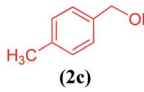 (2c)	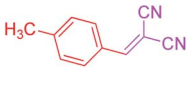 (4c)	16	86
4	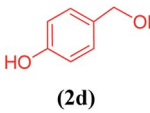 (2d)	 (4d)	13	78
5	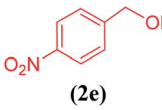 (2e)	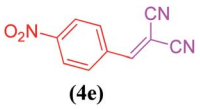 (4e)	10	85
6	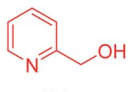 (2f)	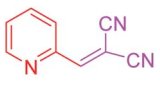 (4f)	15	88
7	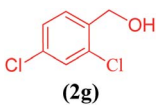 (2g)	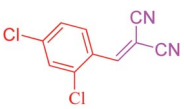 (4g)	8	91

[a] Reaction conditions: benzyl alcohol (**2**, 1 mmol), TBHP (1 mmol), and Cu@EDTAD-PMO (**1**, 4.2 mol%) were added into CH_3CN (2 mL) and stirred at 50 °C. Then, malononitrile (**3**, 1.1 mmol) was added to the reaction mixture.

destruction.[73,74] Hence, lower yield of the desired product **4a** can be assigned to the more affinity of OH radicals to degrade EDTA units in the structure of the Cu@EDTAD-PMO (**1**) rather than the oxidation of benzyl alcohol (Table 1, entry 7). Therefore, TBHP was utilized in the subsequent optimization experiments. It should be noted that the yield of desired product was the same at room temperature and 50 °C, except that longer reaction time was

Table 3 Comparison of the catalytic activity of Cu@EDTAD-PMO (**1**) with other reported catalysts for the synthesis of 2-benzylidenemalononitrile (**2a**)

Entry	Catalyst	Catalyst loading	Oxidant	Temperature (°C)	Time (h)	Yield (%)	References
1	Cu_3TATAT MOF	8 mol%	TEMPO	75	12	90	82
2	Au@MIL-53(NH_2)	(1.0 mol% of Au)	O_2	100	13	99	83
3	Cs–Pr–Me–Cu(II)–Fe_3O_4	20 mg	TBHP	r.t	8	87	63
4	Fe_3O_4@SiO_2@PEI@Ru(OH)$_x$	100 mg	O_2	110	22	91	84
5	**Cu@EDTAD-PMO (1)**	**20 mg (4.2 mol%)**	**TBHP**	**50**	**6**	**95**	**This work**

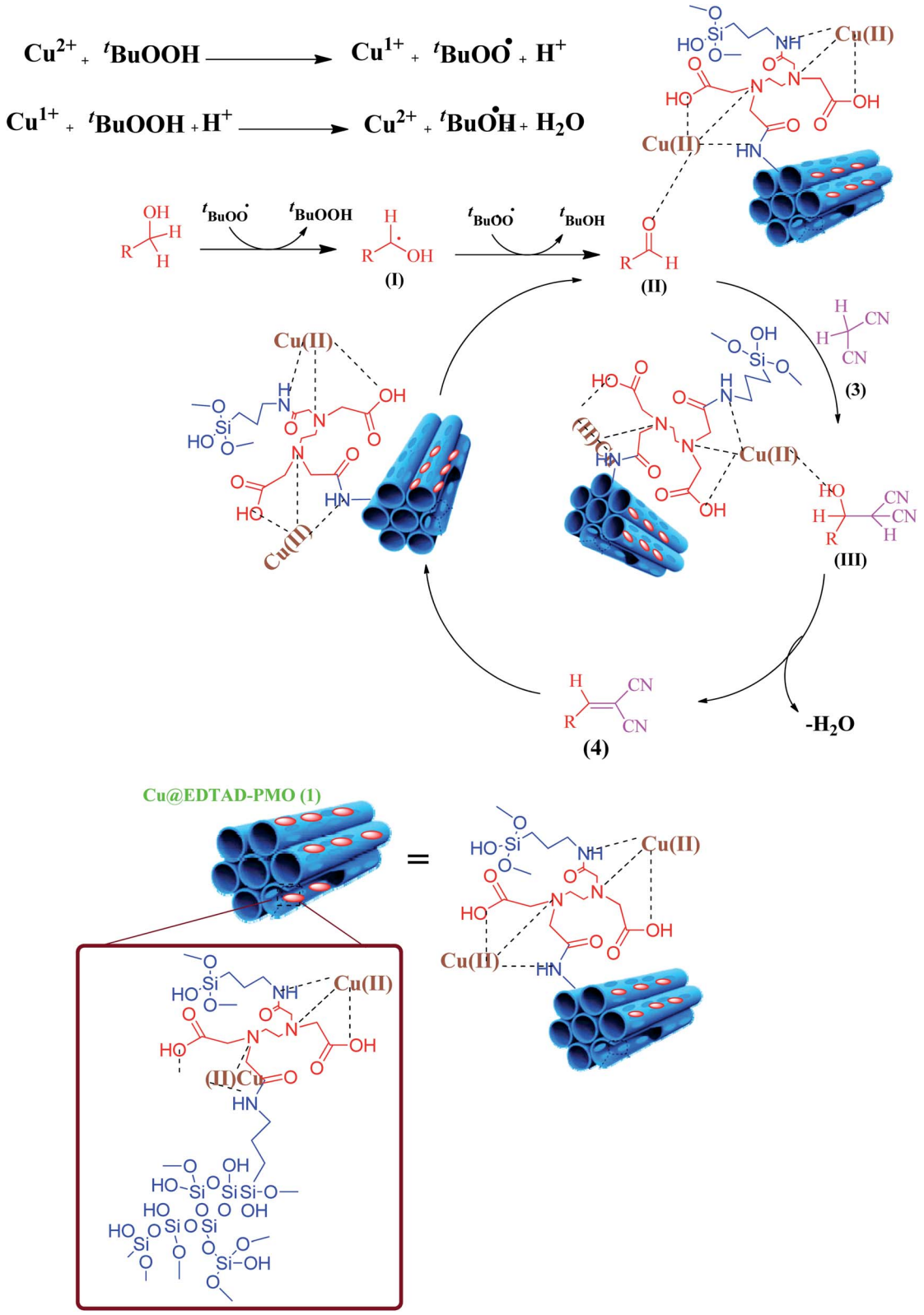

Scheme 2 A plausible mechanism for the oxidation/Knoevenagel condensation of benzyl alcohols in the presence of Cu@EDTAD-PMO catalyst (1).

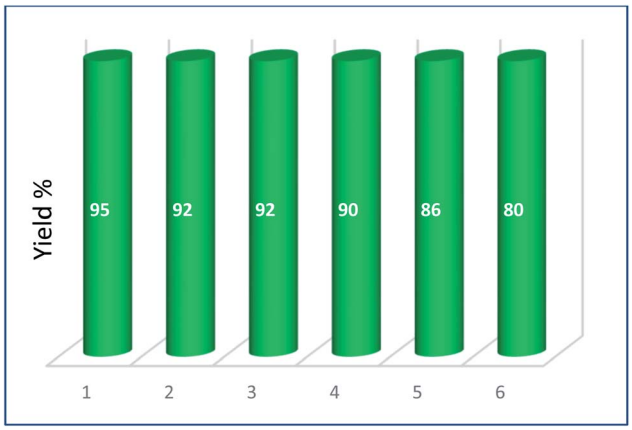

Fig. 8 Reusability of the Cu@EDTAD-PMO catalyst (**1**) in the model reaction.

needed at room temperature (Table 1, entries 8, 9). Therefore, 50 °C was chosen as the optimal temperature for the reaction. In addition, the solvent showed a considerable impact on the oxidation of benzyl alcohol (**2a**) and the subsequent Knoevenagel condensation. For example, in H_2O and toluene, the desired product **4a** was obtained in lower efficiencies than CH_3CN using the same amount of catalyst, even at longer reaction times (Table 1, entries 10, 11). By increasing the amount of catalyst from 1.1 to 4.2 mol%, the conversion of benzyl alcohol (**2a**) to 2-benzylidenemalononitrile (**4a**) significantly increased (Table 1, entries 7, 12–14). Therefore, 4.2 mol% (20 mg) loading of Cu@EDTAD-PMO (**1**) in CH_3CN solvent at 50 °C in the presence of TBHP were determined as the optimal reaction conditions. On the other hand, copper acetate was used at 4.2 mol% catalyst loading under similar conditions to the optimized conditions using Cu@EDTAD-PMO catalyst. However, a lower yield of the desired product **4a** was obtained (Table 1, entry 15).

In order to extend the application of Cu@EDTAD-PMO (**1**), the effect of substrate was also studied under optimal conditions (Table 2). As can be seen, the reaction conditions were compatible with both electron acceptor and electron donor substituents on the aromatic ring. Interestingly, 2-benzylidenemalononitrile (**2a**) could be obtained with 95% yield. In addition, alcohols such as 4-nitrobenzyl alcohol (**2d**) and 4-hydroxybenzyl alcohol (**2e**) reacted slowly to form the corresponding aldehydes in good yield.

Based on the above observations, a free radical mechanism is proposed for the cascade oxidation/Knoevenagel condensation of benzyl alcohols in the presence of Cu@EDTAD-PMO catalyst (**1**) (Scheme 2).[75] First, TBHP is degraded to the *t*-butylproxide radical and proton by reduction of Cu^{2+} ions. The abstraction of a hydrogen radical from benzyl alcohol derivatives **2** produces benzyl radicals (**I**) which can react later with *t*-butylproxide radical to form the corresponding benzaldehyde (**II**) and regenerate Cu(II) species.[76–78] In the next step, aromatic aldehydes and malononitrile (**3**) are activated by the acidic sites of catalyst **1**, respectively *via* a typical Knoevenagel condensation pathway. Eventually, the removal of one water molecule results in the desired products (**4a–f**).[79,80]

One of the advantages of Cu@EDTAD-PMO (**1**) is that it is easily separated from the reaction mixture and can be reused for the next catalytic cycle. As a result, the reusability of the Cu@EDTAD-PMO (**1**) was studied up to the five cycles (Fig. 8). Hence, catalyst **1** was separated from the reaction mixture *via* filtration, washed with hexane, and dried in an oven. Then, it was used again for the cascade oxidation/Knoevenagel condensation reactions. This process was repeated five times without a noticeable decrease in its catalytic efficiency (Fig. 8).

To illustrate the catalytic efficiency of Cu@EDTAD-PMO (**1**) for the oxidation/Knoevenagel condensation of benzyl alcohol with malononitrile, its performance has been compared with different catalytic systems. The results are summarized in Table 3. It is obvious that Cu@EDTAD-PMO (**1**) requires low loading of a low-cost and supported non-toxic transition metal on a novel PMO that can operate at 50 °C to promote one-pot oxidation/Knoevenagel condensation efficiently.

Experimental section

Reagents and apparatus

All chemicals were purchased from Merck or Aldrich with high purity and utilized as received without further purification. Characterization of the mesoporous Cu@EDTAD-PMO nanomaterial was performed by FESEM (TESCAN-MIRA3), EDX (Numerix DXP-X10P), HRTEM (FEI TECNAI F20), FTIR (Shimadzu 8400s), BET (ASAP 2020 micromeritics) and TGA (Bahr Company STA 504). XRD patterns of the mesoporous Cu@EDTAD-PMO nanomaterial were obtained using TW 1800 diffractometer with Cu_{Ka} radiation ($\lambda = 1.54050$ Å). ^{1}H NMR and ^{13}C NMR (500 MHz, Bruker DRX-500 Avance spectrometer in $CDCl_3$) spectral data were compared with those obtained from authentic samples or reported in the literature. Distilled water was utilized in all experiments.

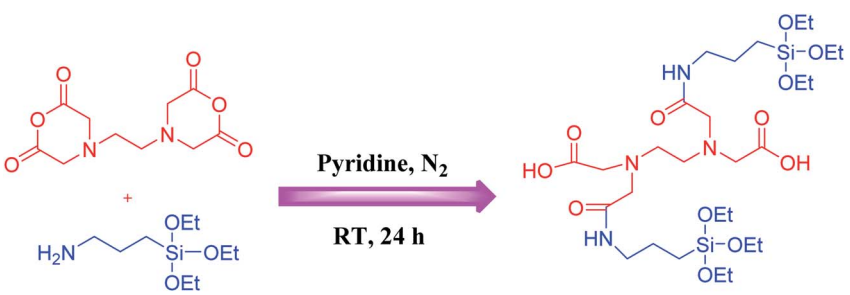

Scheme 3 Preparation of EDTAD-3-(triethoxysilyl)propylamine (**I**).

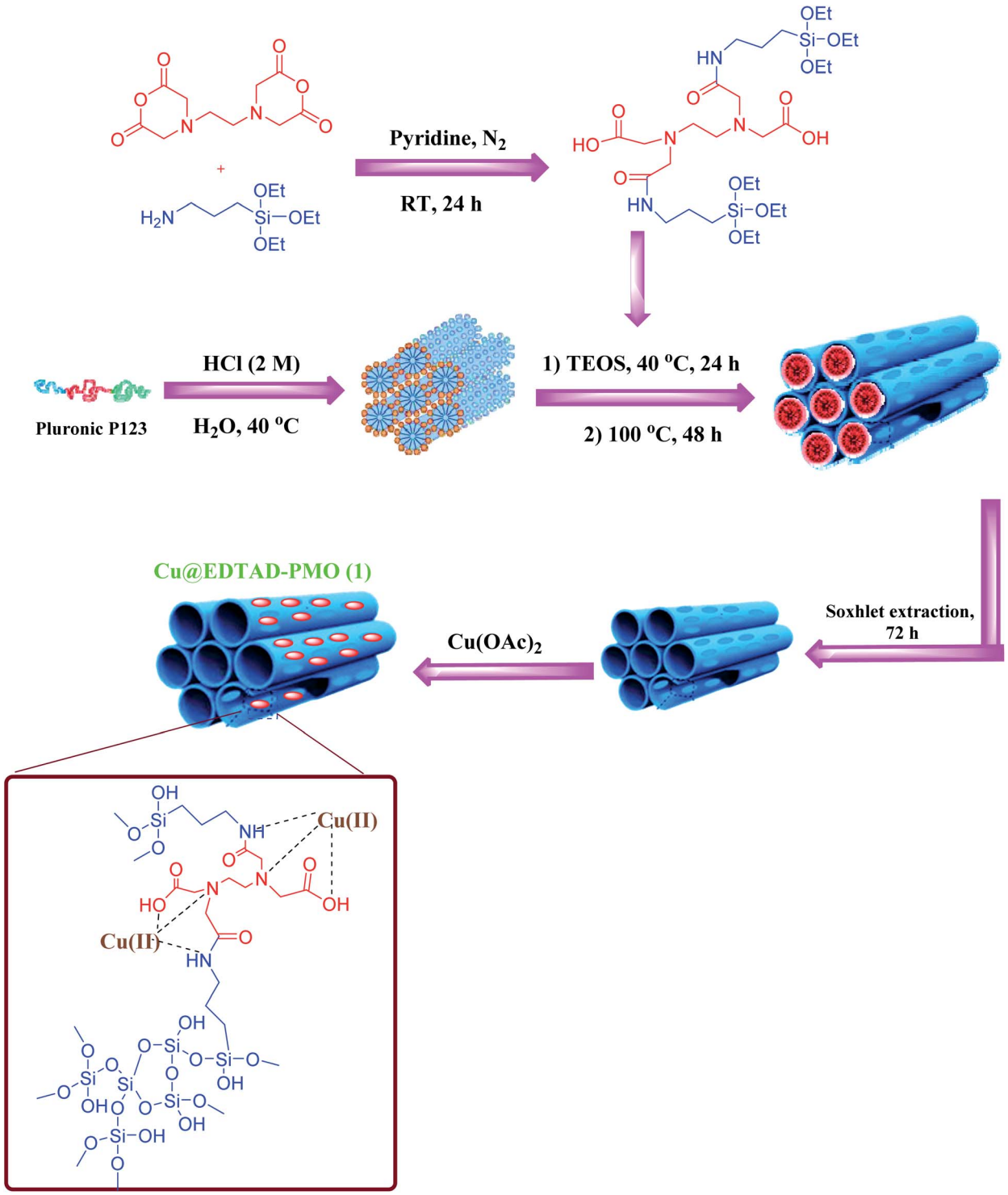

Scheme 4 Schematic preparation of the Cu@EDTAD-PMO nanomaterial (**1**).

General procedure for the preparation of EDTAD-3-(triethoxysilyl)propylamine

EDTA dianhydride (EDTAD, 2 mmol) was dissolved in anhydrous pyridine (10 mL). Then, 3-(triethoxysilyl)propylamine (APTS, 4.5 mmol) was added dropwise into the solution. The resultant reaction mixture was stirred under N_2 atmosphere for 24 h. Eventually, the product was precipitated with hexane, and isolated by centrifugation, then washed with hexane, and dried in 60 °C for 6 h (Scheme 3).[81]

General procedure for the preparation of EDTAD-PMO

Pluronic P123 (1.2 g) was dissolved in a mixture of HCl (43 mL, 2 M) and distilled H_2O (10 mL). Then, the mixture was stirred at room temperature for 4 h and subsequently at 40 °C for 6 h.

Next, EDTAD-APS (**I**, 0.55 g) was added to the mixture and stirred for 30 min. After that, tetraethyl orthosilicate (TEOS, 2.8 mL) was added dropwise and stirred at 40 °C for 24 h, and was then increased to 100 °C and aged at this temperature for 48 h without stirring. Finally, the white precipitate was separated from the mixture, washed with distilled water and EtOH, and dried at 80 °C for 6 h.[85,86] In the following, the product obtained in acidic medium was under Soxhlet extraction conditions using EtOH, as solvent, for 72 h.

General procedure for the preparation of Cu@EDTAD-PMO catalyst (1)

EDTAD-PMO (0.5 g) was dispersed in 10 mL distilled water, then $Cu(OAc)_2$ (0.5 g) was added slowly and stirred at room temperature for 24 h. Then, the mixture was filtered, washed with H_2O and EtOH, and dried at 60 °C for 5 h (Scheme 4).

General procedure for the synthesis of α,β-unsaturated nitriles (4a–f) through cascade oxidation of benzyl alcohols and Knoevenagel condensation catalyzed by Cu@EDTAD-PMO catalyst (1)

In a round-bottomed flask, benzyl alcohol (**2**, 1 mmol), TBHP (1 mmol), and Cu@EDTAD-PMO (**1**, 4.2 mol%) were dissolved in CH_3CN (2 mL) and stirred at 50 °C. Then, malononitrile (**3**, 1.1 mmol) was added to the reaction mixture and stirred for different times reported in Table 2. After reaction completion, the solvent was evaporated. Then, EtOAc (3 mL) was added to the mixture and the Cu@EDTAD-PMO (**1**) was filtered. Next, *n*-hexane was added dropwise into the solution untill benzylidinemalononitrile **4a–f** was completely precipitated. The obtained precipitate was filtered, washed with *n*-hexane, and dried at 70 °C for 3 h. The recycled catalyst **1** was washed with EtOH and hexane and then dried at 50 °C for 2 h.

Spectral characterization of compounds 2c and 2g

2-(4-Methylbenzylidene)malononitrile (2c). FTIR (KBr, cm^{-1}): 3034, 2962, 2223, 1581, 1554, 1485; ^{1}H NMR (500 MHz, $CDCl_3$): δ (ppm) 7.8 (d, $J = 8.0$ Hz, 2H), 7.72 (s, 1H), 7.3 (d, $J = 8.0$ Hz, 2H), 2.47 (Me, 3H); ^{13}C NMR (125 MHz, $CDCl_3$) δ (ppm) 160.8, 146.4, 130.9, 130.3, 128.4, 114, 112.8, 81.1, 22.0.

2-(2,4-Dicholorobenzylidene)malononitrile (2g). FTIR (KBr, cm^{-1}): 3097, 3043, 2227, 1577, 1546, 1461; ^{1}H NMR (500 MHz, $CDCl_3$): δ (ppm) 8.19 (s, 1H), 8.15 (d, $J = 8.5$ Hz, 1H), 7.5 (s, 1H), 7.4 (d, $J = 8.5$ Hz, 1H); ^{13}C NMR (125 MHz, $CDCl_3$) δ (ppm) 159.8, 154.6, 141, 137.1, 130.7, 130.2, 128.3, 127.5, 113.0, 111.8, 85.9.

Conclusions

In summary, a cost-effective and practical route was designed for the facile and rapid synthesis of Cu@EDTAD-PMO with diamide–diacid bridges. The new Cu@EDTAD-PMO catalyst was characterized and used, as a reusable catalyst, for the sustainable cascade oxidation/Knoevenagel condensation of benzyl alcohols to produce corresponding α,β-unsaturated nitriles using TBHP under mild conditions. It was found that high conversion of benzyl alcohols with good selectivities are achievable by using the nano-ordered and reusable Cu@EDTAD-PMO catalyst up to six cycles under mild reaction conditions.

Conflicts of interest

There are no conflicts to declare.

Acknowledgements

We are grateful for the financial support from The Research Council of Iran University of Science and Technology (IUST), Tehran, Iran (Grant No. 160/19810) for their support. We would also like to acknowledge the support of The Iran Nanotechnology Initiative Council (INIC), Iran.

References

1 G. Prieto, H. Tüysüz, N. Duyckaerts, J. Knossalla, G.-H. Wang and F. Schüth, *Chem. Rev.*, 2016, **116**, 14056–14119.
2 X. Li, F. Zhang and D. Zhao, *Chem. Soc. Rev.*, 2015, **44**, 1346–1378.
3 C. Wang, F. Wang, Z. Liu, Y. Zhao, Y. Liu, Q. Yue, H. Zhu, Y. Deng, Y. Wu and D. Zhao, *Nano Energy*, 2017, **41**, 674–680.
4 B. Kong, J. Tang, Y. Zhang, T. Jiang, X. Gong, C. Peng, J. Wei, J. Yang, Y. Wang and X. Wang, *Nat. Chem.*, 2016, **8**, 171–178.
5 B. Kong, J. Tang, Y. Zhang, C. Selomulya, X. Gong, Y. Liu, W. Zhang, J. Yang, W. Wang and X. Sun, *J. Am. Chem. Soc.*, 2015, **137**, 4260–4266.
6 Z. Alirezvani, M. G. Dekamin and E. Valiey, *ACS Omega*, 2019, **4**, 20618–20633.
7 M. Ishani, M. G. Dekamin and Z. Alirezvani, *J. Colloid Interface Sci.*, 2018, **521**, 232–241.
8 F. Jalili, M. Zarei, M. A. Zolfigol, S. Rostamnia and A. R. Moosavi-Zare, *Microporous Mesoporous Mater.*, 2020, **294**, 109865.
9 E. Ali, M. Naimi-Jamal and M. Dekamin, *Sci. Iran.*, 2013, **20**, 592–597.
10 D. Elhamifar, P. Badin and G. Karimipoor, *J. Colloid Interface Sci.*, 2017, **499**, 120–127.
11 J. H. Clark, D. J. Macquarrie and S. J. Tavener, *Dalton Trans.*, 2006, 4297–4309.
12 G. Akay and K. Zhang, *Ind. Eng. Chem. Res.*, 2017, **56**, 457–468.
13 M. Eslami, M. G. Dekamin, L. Motlagh and A. Maleki, *Green Chem. Lett. Rev.*, 2018, **11**, 36–46.
14 E. Valiey and M. G. Dekamin, *Nanoscale Adv.*, 2022, **4**, DOI: 10.1039/d1na00738f.
15 L. Chen, X. Zhou, W. Nie, Q. Zhang, W. Wang, Y. Zhang and C. He, *ACS Appl. Mater. Interfaces*, 2016, **8**, 33829–33841.
16 Y. Cui, Y. H. Lee and J. W. Yang, *Sci. Rep.*, 2017, **7**, 1–9.
17 M. Naeim-Abadi, S. Javanshir, A. Maleki and M. G. Dekamin, *Sci. Iran.*, 2016, **23**, 2724–2734.
18 A. A. Amiri, S. Javanshir, Z. Dolatkhah and M. G. Dekamin, *New J. Chem.*, 2015, **39**, 9665–9671.

19 C. Baleizão, B. Gigante, D. Das, M. Álvaro, H. Garcia and A. Corma, *J. Catal.*, 2004, **223**, 106–113.
20 B. Karimi, D. Elhamifar, J. H. Clark and A. J. Hunt, *Org. Biomol. Chem.*, 2011, **9**, 7420–7426.
21 S. Qiu, H. Zhou, Z. Shen, L. Hao, H. Chen and X. Zhou, *RSC Adv.*, 2020, **10**, 2767–2785.
22 S. Inagaki, S. Guan, Y. Fukushima, T. Ohsuna and O. Terasaki, *J. Am. Chem. Soc.*, 1999, **121**, 9611–9614.
23 T. Asefa, M. J. MacLachlan, N. Coombs and G. A. Ozin, *Nature*, 1999, **402**, 867–871.
24 B. J. Melde, B. T. Holland, C. F. Blanford and A. Stein, *Chem. Mater.*, 1999, **11**, 3302–3308.
25 A. Corma, D. Das, H. García and A. Leyva, *J. Catal.*, 2005, **229**, 322–331.
26 B. Karimi, A. Bigdeli, A. A. Safari, M. Khorasani, H. Vali and S. Khodadadi Karimvand, *ACS Comb. Sci.*, 2020, **22**, 70–79.
27 G. Bagherzade, *RSC Adv.*, 2021, **11**, 19203–19220.
28 T. R. Bastami and Z. Dabirifar, *RSC Adv.*, 2020, **10**, 35949–35956.
29 A. Yaghoubi and M. G. Dekamin, *ChemistrySelect*, 2017, **2**, 9236–9243.
30 M. G. Dekamin, E. Arefi and A. Yaghoubi, *RSC Adv.*, 2016, **6**, 86982–86988.
31 A. Zebardasti, M. G. Dekamin, E. Doustkhah and M. H. N. Assadi, *Inorg. Chem.*, 2020, **59**, 11223–11227.
32 A. Akbari, M. G. Dekamin, A. Yaghoubi and M. R. Naimi-Jamal, *Sci. Rep.*, 2020, **10**, 1–16.
33 A. Yaghoubi, M. G. Dekamin, E. Arefi and B. Karimi, *J. Colloid Interface Sci.*, 2017, **505**, 956–963.
34 P. Van Der Voort, D. Esquivel, E. De Canck, F. Goethals, I. Van Driessche and F. J. Romero-Salguero, *Chem. Soc. Rev.*, 2013, **42**, 3913–3955.
35 J. G. Croissant, Y. Fatieiev, A. Almalik and N. M. Khashab, *Adv. Healthcare Mater.*, 2018, **7**, 1700831.
36 C.-S. Ha and S. S. Park, in *Periodic Mesoporous Organosilicas: Preparation, Properties and Applications*, ed. C.-S. Ha and S. S. Park, Springer Singapore, Singapore, 2019, pp. 125–187, DOI: 10.1007/978-981-13-2959-3_5.
37 A. Akbari, M. G. Dekamin, A. Yaghoubi and M. R. Naimi-Jamal, *Sci. Rep.*, 2020, **10**, 10646.
38 J. Liu, H. Q. Yang, F. Kleitz, Z. G. Chen, T. Yang, E. Strounina, G. Q. Lu and S. Z. Qiao, *Adv. Funct. Mater.*, 2012, **22**, 661.
39 A. Yaghoubi, M. G. Dekamin, E. Arefi and B. Karimi, *J. Colloid Interface Sci.*, 2017, **505**, 956–963.
40 A. Zebardasti, M. G. Dekamin and E. Doustkhah, *Catalysts*, 2021, **11**, 621.
41 J. Yu, M. Tong, X. Sun and B. Li, *Bioresour. Technol.*, 2008, **99**, 2588–2593.
42 C. J. Madadrang, H. Y. Kim, G. Gao, N. Wang, J. Zhu, H. Feng, M. Gorring, M. L. Kasner and S. Hou, *ACS Appl. Mater. Interfaces*, 2012, **4**, 1186–1193.
43 F. Zhao, E. Repo, D. Yin, L. Chen, S. Kalliola, J. Tang, E. Iakovleva, K. C. Tam and M. Sillanpää, *Sci. Rep.*, 2017, **7**, 1–14.
44 E. Repo, J. K. Warchol, T. A. Kurniawan and M. E. Sillanpää, *Chem. Eng. J.*, 2010, **161**, 73–82.
45 Y. Peng, H. Huang, Y. Zhang, C. Kang, S. Chen, L. Song, D. Liu and C. Zhong, *Nat. Commun.*, 2018, **9**, 1–9.
46 S. Ravi, S. Zhang, Y.-R. Lee, K.-K. Kang, J.-M. Kim, J.-W. Ahn and W.-S. Ahn, *J. Ind. Eng. Chem.*, 2018, **67**, 210–218.
47 Y. Hayashi, *Chem. Sci.*, 2016, **7**, 866–880.
48 Q. Yang, H.-Y. Zhang, L. Wang, Y. Zhang and J. Zhao, *ACS Omega*, 2018, **3**, 4199–4212.
49 H. Wang, C. Wang, Y. Yang, M. Zhao and Y. Wang, *Catal. Sci. Technol.*, 2017, **7**, 405–417.
50 D. Elhamifar, O. Yari and B. Karimi, *J. Colloid Interface Sci.*, 2017, **500**, 212–219.
51 M. A. Zolfigol, F. Shirini, G. Chehardoli and E. Kolvari, *J. Mol. Catal. A: Chem.*, 2007, **265**, 272–275.
52 M. Mahyari and A. Shaabani, *Appl. Catal., A*, 2014, **469**, 524–531.
53 X. Garrabou, B. I. Wicky and D. Hilvert, *J. Am. Chem. Soc.*, 2016, **138**, 6972–6974.
54 S. Bi, C. Yang, W. Zhang, J. Xu, L. Liu, D. Wu, X. Wang, Y. Han, Q. Liang and F. Zhang, *Nat. Commun.*, 2019, **10**, 1–10.
55 M. G. Dekamin, M. Eslami and A. Maleki, *Tetrahedron*, 2013, **69**, 1074–1085.
56 Z. Alirezvani, M. G. Dekamin, F. Davoodi and E. Valiey, *ChemistrySelect*, 2018, **3**, 10450–10463.
57 A. Ying, Y. Ni, S. Xu, S. Liu, J. Yang and R. Li, *Ind. Eng. Chem. Res.*, 2014, **53**, 5678–5682.
58 Y. Guo, L. Feng, C. Wu, X. Wang and X. Zhang, *ACS Appl. Mater. Interfaces*, 2019, **11**, 33978–33986.
59 W. Piao, Z. Li, C. Li, J. S. Park, J.-h. Lee, Z. Li, K. Y. Kim, L. Y. Jin, J. M. Kim and M. Jin, *RSC Adv.*, 2021, **11**, 27453–27460.
60 Z. Alirezvani, M. G. Dekamin and E. Valiey, *Sci. Rep.*, 2019, **9**, 17758.
61 D. Wang and Z. Li, *Catal. Sci. Technol.*, 2015, **5**, 1623–1628.
62 W. Zhou, S. Zhai, J. Pan, A. Cui, J. Qian, M. He, Z. Xu and Q. Chen, *Asian J. Org. Chem.*, 2017, **6**, 1536–1541.
63 Z. Alirezvani, M. G. Dekamin and E. Valiey, *Sci. Rep.*, 2019, **9**, 1–12.
64 M. A. Hussain, M. Irshad, E. U. Haq, S. Park, M. Atif, A. S. Hakeem, B. G. Choi and J. W. Kim, *Ind. Eng. Chem. Res.*, 2019, **58**, 23025–23031.
65 N. Azizi, M. Khajeh and M. Alipour, *Ind. Eng. Chem. Res.*, 2014, **53**, 15561–15565.
66 W. Jiang, J. Yang, Y.-Y. Liu, S.-Y. Song and J.-F. Ma, *Inorg. Chem.*, 2017, **56**, 3036–3043.
67 S. L. Scott, A. Bakac and J. H. Espenson, *J. Am. Chem. Soc.*, 1992, **114**, 4205–4213.
68 D. B. Dess and J. Martin, *J. Am. Chem. Soc.*, 1991, **113**, 7277–7287.
69 N. Ghanbari, H. Ghafuri and H. R. E. Zand, *ChemistrySelect*, 2018, **3**, 3394–3399.
70 A. Shaabani, A. T. Tabatabaei, F. Hajishaabanha, S. Shaabani, M. Seyyedhamzeh and M. Keramati nejad, *J. Sulfur Chem.*, 2018, **39**, 367–379.
71 B. Karimi, D. Elhamifar, J. H. Clark and A. J. Hunt, *Chem.–Eur. J.*, 2010, **16**, 8047–8053.
72 M. Kruk and M. Jaroniec, *Chem. Mater.*, 2001, **13**, 3169–3183.
73 J. Rämö and M. Sillanpää, *J. Cleaner Prod.*, 2001, **9**, 191–195.

74 A. Kunz, P. Peralta-Zamora and N. Durán, *Adv. Environ. Res.*, 2002, **7**, 197–202.
75 E. Doustkhah, H. Mohtasham, M. Hasani, Y. Ide, S. Rostamnia, N. Tsunoji and M. H. N. Assadi, *Mol. Catal.*, 2020, **482**, 110676.
76 S. Rostamnia, E. Doustkhah, Z. Karimi, S. Amini and R. Luque, *ChemCatChem*, 2015, **7**, 1678–1683.
77 A. Dutta, M. Chetia, A. A. Ali, A. Bordoloi, P. S. Gehlot, A. Kumar and D. Sarma, *Catal. Lett.*, 2019, **149**, 141–150.
78 M. J. Nejad, A. Salamatmanesh and A. Heydari, *J. Organomet. Chem.*, 2020, **911**, 121128.
79 T. Rahman, G. Borah and P. K. Gogoi, *J. Chem. Sci.*, 2019, **131**, 1–9.
80 N. Gogoi, T. Begum, S. Dutta, U. Bora and P. K. Gogoi, *RSC Adv.*, 2015, **5**, 95344–95352.
81 D. Patel, A. Kell, B. Simard, J. Deng, B. Xiang, H.-Y. Lin, M. Gruwel and G. Tian, *Biomaterials*, 2010, **31**, 2866–2873.
82 Z. Miao, Y. Luan, C. Qi and D. Ramella, *Dalton Trans.*, 2016, **45**, 13917–13924.
83 Y. Qi, Y. Luan, X. Peng, M. Yang, J. Hou and G. Wang, *Eur. J. Inorg. Chem.*, 2015, **2015**, 5099–5105.
84 H. Yan, H.-Y. Zhang, L. Wang, Y. Zhang and J. Zhao, *React. Kinet., Mech. Catal.*, 2018, **125**, 789–806.
85 A. Ahadi, S. Rostamnia, P. Panahi, L. D. Wilson, Q. Kong, Z. An and M. Shokouhimehr, *Catalysts*, 2019, **9**, 140.
86 M. Esmat, H. Mohtasham, Y. GadelHak, R. T. Mehrebani, R. Tahawy, S. Rostamnia, N. Fukata, S. Khaksar and E. Doustkhah, *Catalysts*, 2020, **10**, 167.